Template-free synthesis of $Nd_{0.1}Bi_{0.9}FeO_3$ nanotubes with large inner diameter and wasp-waisted hysteresis loop

X. Li,[1] F. Guo,[1] S. Y. Wang,[1,2,a)] X. Wang,[1] X. L. Xu,[3] J. Gao,[2] and W. F. Liu[3,a)]
[1]*College of Physics and Material Science, Tianjin Normal University, Tianjin 300074, China*
[2]*Department of Physics, The University of Hong Kong, Pokfulam Road, Hong Kong*
[3]*Tianjin Key Laboratory of Low Dimensional Materials Physics and Preparing Technology, Faculty of Science, Tianjin University, Tianjin 300072, China*

(Received 28 April 2015; accepted 2 August 2015; published online 11 August 2015)

One-dimensional (1D) nanotubes of $Nd_{0.1}Bi_{0.9}FeO_3$ (NBFO) with an inner diameter of ~50 nm were synthesized via sol-gel based electrospinning without template assistant. The phases, morphologies, crystalline structures, and magnetic properties of these 1D nanostructures were characterized by means of X-ray diffraction, scanning electron microscopy, transmission electron microscopy and SQUID, respectively. It was found that the calcination condition plays a crucial role in determining the morphologies and the magnetic properties. Interestingly, these 1D NBFO nanotubes exhibit wasp-waisted magnetic hysteresis with a lower coercivity and larger saturation magnetization, which were prevalent in natural rocks and artificial composite materials. The origin of these wasp-waisted hysteresis loops was discussed. © *2015 AIP Publishing LLC*.
[http://dx.doi.org/10.1063/1.4928546]

Hysteresis loops give information concerning the coercivity spectrum and domain state of ferri- and ferromagnetic materials. Wasp-waisted hysteresis loops, which are constricted in the middle section, were first described in the 1920s by Gumlich.[1] Since then, examples of wasp-waisted hysteresis loops were reported widely in the Y-type hexagonal ferrite, as well as in composite materials, such as $FeO@BaTiO_3$ with core shell structure, and rock samples.[2–4] The wasp-waisted shape is thought to arise from the grain's dispersed distribution of sizes, domain states, and coercive fields.[3–5] However, wasp-waisted hysteresis loop has rarely been observed in one-dimensional (1D) nanomaterial, although they attract more attention due to the distinctive properties compared with their bulk or particle counterparts.

As one of the most promising multiferroic materials, $BiFeO_3$ (BFO) is known for its unique feature that can show both ferroelectric ($T_C \sim 1103$ K) and antiferromagnetic ($T_N \sim 643$ K) at room temperature.[6–9] Recent work has suggested that 1D BFO nanowires (NWs) exhibit enhanced ferromagnetic ordering and the magneto crystalline anisotropy, as well as increased ferromagnetism with smaller particle size.[8–12] Comparing with NWs, nanotubes (NTs) may present additional degree of freedom, due to the variation in their length, radius, and the wall-thickness. A few groups have reported the synthesis of BFO NTs with a sol-gel anodic alumina oxide (AAO) template method.[13–15] However, this template method has some distinct disadvantages including low aspect ratios and the diffusion of aluminum ions into NTs causing heterogeneous impurities. Comparison with AAO method, electrospinning (ES) has been widely adopted for the preparation of various 1D nanomaterial because of its simplicity, low cost, and relatively high production rate. There are some people who have observed the electro-optical properties in 1D BFO nanostructures in the past decade.[16] However, the magnetic property of BFO NTs synthesized by employing the ES route has rarely been reported. Both theoretical predictions and experimental investigations suggest that the magnetic properties in BFO NTs might be significantly improved with reduced dimensions and enhanced ratio of surface to volume.[17]

Among various kinds of methods to improve the multiferroic properties, doping with rare earth ions at Bi site of BFO is an effective way to achieve higher magnetic moment and large magnetic coupling. Moreover, in our previous work, it was found that 10% Nd doping in $Bi_{1-x}Nd_xFeO_3$ nanoparticles could lead to a ferromagnetic phase with a relative larger magnetization and higher insulating resistivity.[18] In this work, we report a technique by employing facile ES with a delicate calcination process to obtain 1D $Nd_{0.1}Bi_{0.9}FeO_3$ (NBFO) NTs with outer diameter of 100–150 nm and large inner diameter of 40–80 nm. Moreover, wasp-waisted M-H loops with a low coercivity and larger saturation magnetization were observed in these NBFO NTs. The correlation of microstructure with their magnetic properties and morphologies of NBFO NTs was elucidated in detail. This study shows a way to obtain high-performance 1D multiferroic materials and may provide insight into the physics of NBFO NTs.

NBFO samples were synthesized using a sol-gel based ES method. Bismuth nitrate, neodymium nitride, and iron nitrate were dissolved in DMF (N-N-dimethylformamide, C_3H_7NO) to prepare sol-gel solution. The ES process was performed at a voltage of 15 kV and a feed rate of 0.3 ml/h with 10 cm spacing between the needle tip and collector. The electro spun polymer composite nanofibers (NFs) were collected using an alumina crucible and heated at 280 °C for 1 h first, and then were increased to the designed calcination temperature of 400–600 °C with a heating rate of 1 °C/min. At the specified temperature, the as-spun NBFO NFs were calcined for 2 h in air, followed by a natural cooling procedure

a)Authors to whom correspondence should be addressed. Electronic addresses: shouyu.wang@yahoo.com, Tel./Fax: +86 22 23766503 and wfliu@tju.edu.cn, Tel./Fax: +86 22 23766503.

 © 2015 AIP Publishing LLC

This article is copyrighted as indicated in the article. Reuse of AIP content is subject to the terms at: http://scitation.aip.org/termsconditions. Downloaded to IP: 147.8.31.43 On: Wed, 23 Sep 2015 02:37:27

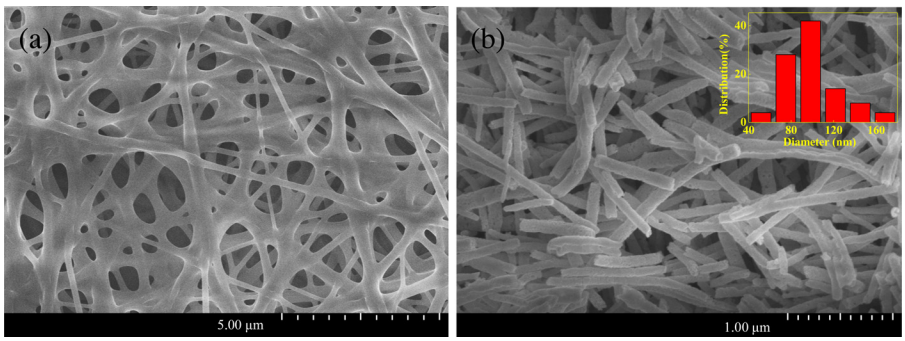

FIG. 1. SEM images of electrospun NBFO composite nanofibers without calcination treatment (a) and after calcination at 400 °C (b), inset of (b) showing the size distribution of diameters in the synthesized NBFO nanotubes.

down to room temperature. The details of synthesis and characterization are presented in the supplementary material.[19]

The scanning electron microscopy (SEM) images of NBFO NTs without heat treatment are shown in Fig. 1(a). The as-spun fibers have a rather uniform diameter around 200–400 nm over their length with a smooth shape owing to the polymer nature of carrier PVP (polyvinylpyrrolidone). After the sintering process, the NFs remain in 1D structures, while the average diameter shrinks to ~90 nm and their morphology turns to be coarse. A tubular morphology is observed in NBFO, as shown in Fig. 1(b). However, it is hard to observe the tubular morphology in the NBFO calcined at higher temperature (500–600 °C). They show the single-particle-chain like morphology (see supplementary Fig. S1).[19] Such a morphology evolution can be attributed to the thermal decomposition of PVP, the coarsening and coalescence of smaller crystallites of NBFO.

High-resolution transmission electron microscopy (HRTEM) was employed to confirm the tubular morphology and to reveal the crystalline structure of NBFO NTs, as shown in Fig. 2. 1D tubular structure is observed in NBFO NTs with inner diameter of ~45 nm and wall thickness of ~20 nm. Inset of Fig. 2(a) shows the HRTEM and selected area electron diffraction pattern (SAED) taken from representative NTs. The SAED of NBFO NTs presents diffused rings superimposed with spots, demonstrating that NBFO NTs consist of polycrystalline state as well as amorphous state. The crystalline nature and composition of the NTs are further confirmed by the HRTEM images, as shown in Figs. 2(c) and 2(d). The middle area of the NBFO NTs shows local crystalline regions with size ~6 nm embedded in amorphous matrix marked by red rectangular. While for the front areas of NTs, the well-recognized lattice lines are clear. The planes with inter-plane spacing of 0.258 nm and 0.451 nm are corresponding to (211) and (212) crystal faces, respectively. Similar phenomena of coexisting of polycrystalline and amorphous states have been observed in BFO NTs and nanoparticles synthesized with relatively low calcination temperatures.[13,20,21] When the calcination temperature increases to 500–600 °C, these NBFO samples show nanofiber morphology comprising dense circular-like crystalline grains. All corresponding SAED patterns (see supplementary Fig. S2)[19] show very sharp diffraction spots, indicating the single-crystalline characteristics of well developed large-size grains in these NBFO NFs.

Phase purification, chemical bonding, and oxidation states of elements of the NTs were analyzed by X-ray photoelectron spectrum and X-ray diffraction (see supplementary Figs. S3 and S4).[19] Apart from small amount of adsorbed carbon, no any other impurity elements could be detected. Crystal structure characteristics of NTs agree well with our previous observation in Nd-doped BFO nanoparticles and

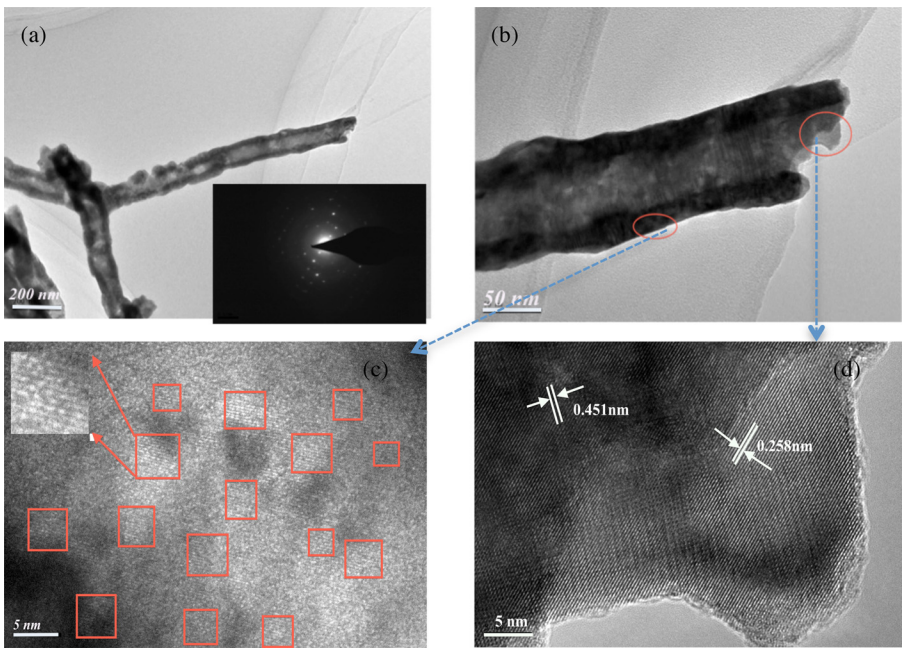

FIG. 2. (a) TEM images of NBFO nanotubes, inset shows the corresponding SAED pattern of a single nanotube; (b) TEM images of a single NBFO nanotube, red circles are used to indicate the areas enlarged by HRTEM; (c) HRTEM image of front area in a single NBFO nanotube; and (d) HRTEM image of middle area in a single NBFO nanotube with local crystallization regions.

This article is copyrighted as indicated in the article. Reuse of AIP content is subject to the terms at: http://scitation.aip.org/termsconditions. Downloaded to IP: 147.8.31.43 On: Wed, 23 Sep 2015 02:37:27

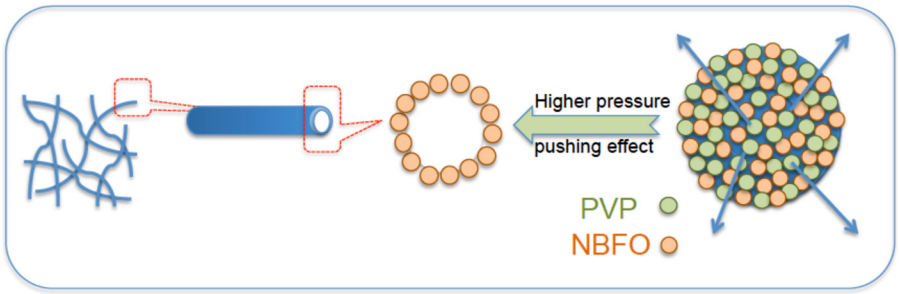

FIG. 3. Schematic diagram of synthesis mechanism of NBFO NTs.

can be ascribed to a larger lattice distortion.[18] Structure parameters (see supplementary Table S1)[19] obtained from Rietveld refinement demonstrate a distorted rhombohedra structure with R3c space group for NBFO NTs.

The formation mechanism of these NBFO NTs with multi-particle-chain can be ascribed to thermally induced phase separation and grain growth.[16,22] For NBFO calcined at 400 °C or 450 °C, the time for the removal of PVP located inside of fiber is longer than that located near the surface, hence the pressure inside the fibers is larger than that outside, which pushes the interior parts of BFO/PVP to move outward, eventually forming hollow spaces in fibers, as shown in Fig. 3. For NBFO calcined at higher temperature (500 °C–600 °C), the transform process of NBFO/PVP still occurs, and simultaneously competes with grain growth and coalescence processes, because the higher calcination temperature facilitates tiny NBFO grains nearby to merge into larger size particles. This results in large grain size in NFs with single-particle-chain morphology, accompanied by a shrink or disappearance of the tubular structure. Therefore, the careful tailoring of calcination process plays a key role in determining nanostructure morphology, as well as magnetic properties of NTs.

It is well known that the magnetic behavior of nanomaterials is strongly affected by grain size, sample shape, crystallinity, etc.[17,23–26] M-H hysteresis loops of NBFO measured at room temperature are shown in Fig. 4, wherein a M-H loop of NBFO NFs (calcined at 500 °C) is also presented to contrast with the NBFO NTs. It can be seen that the NTs show a good saturation of magnetization in contrary to antiferromagnetic bulk BFO, which may be attributed to the size effect and non-exact compensation of two magnetic sublattices in NTs' surface.[11–14] At the maximum field of 5 T, the specific saturation magnetization approaches 1.82 emu/g for NTs, which is 2 times larger in comparison with that of NBFO nanoparticles (NPs) and BFO NTs.[11,18] One reason for the higher saturation magnetization in NBFO NTs lies in their tubular structure with smaller particle size as demonstrated by TEM. Uncompensated surface spins in NTs become more significant due to a large ratio of surface to volume, since the long-range antiferromagnetic order is frequently interrupted at the particle surface.[11–14] Another possible reason is that the FeO_2/FeO_2 terminated surfaces that cover the NTs' surface with relative larger magnetic moment.[26]

The coercivity (H_c) of NBFO NTs is only ~300 Oe (Fig. 4(b)), which is significantly smaller than those values (>1 T) observed in NBFO NFs.[18] Such small H_c for NTs might be due to small particle size, magnetoelastic anisotropy, and magneto–crystalline anisotropy.[18,20] It is worth to note that NBFO NTs exhibit obvious constricted M-H loops characterized by a small coercivity at low fields (H < 1000 Oe), whereas at higher fields (>2000 Oe) these M-H loops are open at both ends. If further raising the field, closing of loops and magnetization saturation could be observed. However, NBFO NFs' M-H loops do not show constricted characteristics, which are analogous with our previous results of NBFO nanoparticles synthesized by sol-gel method.[18] This kind of constricted loop was ever observed in Y-type hexagonal ferrite, and in shape memory alloys, as well as in composite materials, such as $FeO@BaTiO_3$, Fe_2O_3-Fe_3O_4 mixture, or rock samples.[2–5] In present case of NBFO NTs, the most likely origin is the coexistence of magnetic phases with widely different coercivity. As elucidated by HRTEM and XRD, NBFO NTs consist of amorphous phase and polycrystalline state with smaller grain size of ~6 nm. Then, the uncompensated surface spins would become more significant due to the increase of surface to volume ratio, leading to an enhancement of the tangible contribution to overall magnetization and a large distribution of coercivity.[8–12]

In order to distinguish various magnetic component causing wasp-waisted hysteresis, the difference of magnetization (δM) between ascending and descending portions of hysteresis for H > 0 was plotted (top of Fig. 4(b)). For NFs,

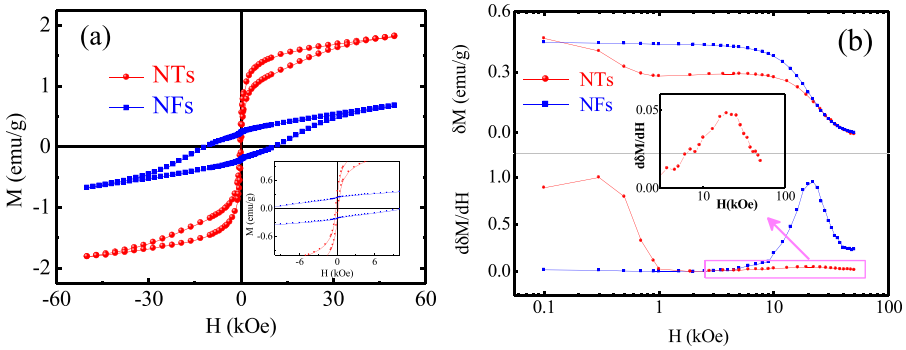

FIG. 4. (a) The field dependent magnetization hysteresis (M-H) loops of NBFO NTs and NFs at room temperature. Inset shows the enlargement range in ±10 kOe. (b).Top shows δM between ascending and descending portions of M-H in (a) for H > 0; the bottom part shows dδM/dB. Inset of (b) shows the enlargement of dδM/dB curve of NBFO NTs from 3 kOe to 100 kOe.

This article is copyrighted as indicated in the article. Reuse of AIP content is subject to the terms at: http://scitation.aip.org/termsconditions. Downloaded to IP: 147.8.31.43 On: Wed, 23 Sep 2015 02:37:27

the δM curves decay slowly with increasing magnetic field for $H < 1$ T, and then rapidly decrease *monotonically*, but do not reach zero until about 4 T. However, for NTs, the initial portion of δM curve decays rapidly to about 0.28 with magnetic field for $H < 0.1$ T. Then, δM become almost constant in intermediate range of magnetic fields. When $H > 1$ T, δM curves show decreasing trend that is analogous with that of NBFO NFs. Both δM curves are nearly overlapped in field range $H > 1.2$ T. The bottom part of Fig. 4(b) shows the derivative of the δM curves (dδM/dH), which can reveal the distribution and content of various coercivities contributing to the remanence more clearly. The dδM/dH curve of NTs exhibits quite different trend compared with that of NFs. For NTs, there are two peaks centered on around 0.3 kOe and 17 kOe in dδM/dH curve. Furthermore, the rise from 0.1 to 0.3 kOe results from purely reversible behavior. Such low-field peak is much higher than that located at higher fields, implying that the low coercivity (soft ferrimagnetic) component dominant for NTs' magnetization. However, for NFs, a relatively obvious large hump centers around 17 kOe in the dδM/dH curve, which is consistent with the monotonic decrease of its corresponding δM curve, demonstrating that the component with higher coercivity is prominent. Therefore, the high-field characteristics should be controlled by the hard component, larger-grain-size NBFO particles, while the lower-field behavior in M-H loops should be controlled by soft component of NBFO grains with smaller size.[3–5] Besides, as shown in XRD results, there is small amount of residual phase of $Bi_2Fe_4O_9$ in NBFO NTs. Tian *et al*. demonstrated that $Bi_2Fe_4O_9$ showed weak ferromagnetic behavior with corresponding coercivity $Hc = 240$ Oe and saturation magnetization $Ms \approx 0.58$ emu/g.[27] This indicates that the residual $Bi_2Fe_4O_9$ maybe a relatively weak contribution to the lower coercivity in NTs' M-H loops. These wasp-waisted hysteresis loops indicate a smaller random-field disorder. In this case, the connectivity of spins at surface of grain/cluster has a larger effect on the hysteresis loops' shape.[5] The observation of an enhanced saturation magnetization and small hysteresis loss in NTs may pave a way for improving magnetic properties of multiferroic BFO.

In conclusion, this work demonstrates the synthesis of 1D NBFO NTs without template assistant, using a facile ES with delicate calcination process. Different crystalline states in 1D NBFO NTs lead to wasp-waisted hysteresis with enhanced saturation magnetism and reduced coercivity. Such NTs with constricted loops may be benefit for designing future nanoscale building blocks for soft magnetic materials for applications in transformers and inductors.

This work was funded by the Research Grant Council of Hong Kong (RGC No. 702112), Key laboratory of Optoelectronic Information Technology, Ministry of Education, China (Tianjin University), and the National Natural Science Foundation of China (Nos. 11374225, 11004148, and 11104202).

[1]E. Gumlich, Arch. Elektrotech. **9**, 153 (1920).
[2]G. Muttoni, Geophys. Res. Lett. **22**, 3167, doi:10.1029/95GL03073 (1995).
[3]L. Tauxe, T. A. T. Mullender, and T. Pick, J. Geophys. Res. **101**, 571, doi:10.1029/95JB03041 (1996).
[4]L. Curecheriu, P. Postolache, M. T. Buscaglia, V. Buscaglia, A. Lanculescu, and L. Mitoseriu, J. Appl. Phys. **116**, 084102 (2014).
[5]R. S. Kharwanlang and P. Shukla, Phys. Rev. E **85**, 011124 (2012).
[6]S. W. Cheong and M. Mostovoy, Nat. Mater. **6**, 13 (2007).
[7]M. Fiebig. J. Phys. D: Appl. Phys. **38**, R123 (2005).
[8]S. H. Xie, J. Y. Li, R. Proksch, Y. M. Liu, Y. C. Zhou, Y. Y. Liu, Y. Ou, L. N. Lan, and Y. Qiao, Appl. Phys. Lett. **93**, 222904 (2008).
[9]F. Gao, X. Y. Chen, and K. B. Yin, Adv. Mater. **19**, 2889 (2007).
[10]X. Y. Zhang, C. W. Lai, X. Zhao, D. Y. Wang, and J. Y. Dai, Appl. Phys. Lett. **87**, 143102 (2005).
[11]A. Jaiswal, R. Das, and K. Vivekanand, J. Phys. Chem. C **114**, 2108 (2010).
[12]T.-J. Park, Y. B. Mao, and S. S. Wong, Chem. Commun. **2004**, 2708–2709.
[13]X. Q. Xu, T. Qian, G. Q. Zhang, T. Zhao, G. Li, W. Wang, and X. G. Li, Chem. Lett. **36**, 112 (2007).
[14]L. A. S. De Oliveira and K. R. Pirota, Mater. Res. Bull. **48**, 1593 (2013).
[15]J. Wang, M. Y. Li, and X. L. Liu, Chin. Sci. Bull. **55**, 1594 (2010).
[16]S. Mohan and B. A. Subramanian, RSC Adv. **3**, 23737 (2013).
[17]X.-F. Han, S. Shamaila, R. Sharif, J.-Y. Chen, H.-R. Liu, and D.-P. Liu, Adv. Mater. **21**, 4619 (2009).
[18]H. Zhang, W. F. Liu, P. Wu, X. Hai, S. Y. Wang, G. Y. Liu, and G. H. Rao, J. Nanoparticle Res. **16**, 2205 (2014).
[19]See supplementary material at http://dx.doi.org/10.1063/1.4928546 for more details on the preparation and XPS, TEM characterization, and XRD Rietveld refinement of NBFO NTs and NFs.
[20]P. S. V. Mocerla, C. Karthik, R. Ubic, M. S. Ramachandra Rao, and C. Sudakar, Appl. Phys. Lett. **105**, 132409 (2014).
[21]Y. N. Feng, H. C. Wang, and Y. D. Luo, J. Appl. Phys. **113**, 146101 (2013).
[22]J. T. McCann, M. Marquez, and Y. N. Xia, J. Amer. Chem. Soc. **128**, 1436 (2006).
[23]T. J. Park, G. C. Papaefthymiou, and A. J. Viescas, Nano Lett. **7**, 766 (2007).
[24]Y. G. Wang, G. Xu, and Z. H. Ren, J. Amer. Ceram. Soc. **90**, 2615 (2007).
[25]A. V. Zalesskii, A. K. Zvezdin, and A. A. Frolov, JETP Lett. **71**, 465 (2000).
[26]M. Sobhan, Q. Xu, Q. Yang, F. Anariba, and P. Wu, Appl. Phys. Lett. **104**, 051606 (2014).
[27]Z. M. Tian, S. L. Yuan, X. L. Wang, X. F. Zheng, S. Y. Yin, C. H. Wang, and L. Liu, J. Appl. Phys. **106**, 103912 (2009).

This article is copyrighted as indicated in the article. Reuse of AIP content is subject to the terms at: http://scitation.aip.org/termsconditions. Downloaded to IP: 147.8.31.43 On: Wed, 23 Sep 2015 02:37:27